IOSR Journal of Computer Engineering (IOSR-JCE)
e-ISSN: 2278-0661, p-ISSN: 2278-8727, Volume 28, Issue 3, Ser. II (May. – June. 2026), PP 45-54
www.iosrjournals.org

Terminal Sliding Mode Position Control for a Load-Sensing Electro-Hydraulic Rotary Actuator

Nguyen Ngoc Tuan, Phung Manh Hung, Tang Thanh Lam, Nguyen Tuan Minh, Nguyen Van Tien, Duong Ngoc Khang, Ngo Viet Cuong, To Xuan Dinh*
Institute of Control Engineering, Le Quy Don Technical University, Hanoi, Vietnam
**Corresponding author, email: dinhtx@lqdtu.edu.vn*

Abstract
This paper presents a terminal sliding mode control approach for position tracking of a servo-valve-controlled electro-hydraulic rotary actuator supplied by a load-sensing hydraulic pump. A nonlinear control-oriented model is formulated by incorporating the main rotary mechanical dynamics, hydraulic pressure dynamics, servo-valve flow characteristics, valve spool dynamics, and load-sensing supply-pressure regulation. Based on this model, a terminal sliding mode controller is developed to improve transient response and tracking accuracy. The nonlinear terminal sliding surface is introduced to enhance convergence behavior, while a continuous saturation function is employed to alleviate chattering in the control input. MATLAB/Simulink simulations are conducted under sinusoidal and rectangular-wave reference trajectories. Comparative results with conventional PID and standard sliding mode controllers demonstrate that the proposed terminal sliding mode controller achieves improved tracking accuracy, faster response, and acceptable control smoothness under the considered operating conditions.

Keywords: *electro-hydraulic rotary actuator terminal sliding mode control; load-sensing pump.*

Date of Submission: 01-06-2026 Date of Acceptance: 10-06-2026

I. INTRODUCTION

High-accuracy motion control under nonlinear dynamics and uncertain operating conditions remains an important problem in modern hydraulic drive systems. In systems requiring reliable angular motion and high load capacity, hydraulic rotary actuators are frequently adopted as compact torque-generation mechanisms. However, their control performance is strongly affected by the coupling among mechanical motion, hydraulic pressure variation, valve-flow characteristics, friction, leakage, and load-dependent effects. These factors make accurate position tracking difficult, particularly when the actuator operates under fast reference changes or varying load conditions [1-2].

Servo-valve-controlled hydraulic rotary actuators are commonly used when precise angular displacement regulation is required. In this configuration, the servo valve regulates the flow entering the actuator chambers, and the resulting pressure difference generates the output torque. Although this structure provides effective controllability, it introduces nonlinear behavior because the valve flow depends simultaneously on spool displacement and pressure drop. In addition, fluid compressibility, internal leakage, friction, and limited valve bandwidth further influence the closed-loop response. Therefore, a suitable controller should maintain tracking accuracy while reducing the effect of these nonlinear characteristics.

Proportional-integral-derivative control is widely used in practical hydraulic systems because of its simple implementation. Nevertheless, fixed-gain linear control often becomes insufficient when the hydraulic parameters vary or when the desired trajectory contains rapid acceleration and direction reversal. To overcome these limitations, nonlinear robust control methods have been investigated for hydraulic and precision motion systems. Sliding mode control is attractive because of its robustness to matched uncertainties and modeling errors. However, conventional sliding mode control generally provides asymptotic convergence, and its discontinuous switching term may produce chattering in the control signal.

Terminal sliding mode control was introduced to improve convergence behavior by using a nonlinear sliding surface [3-4]. This method can provide faster error convergence than conventional linear sliding mode control, making it suitable for position tracking systems that require rapid transient response and small steady-state error. In hydraulic systems, finite-time and terminal sliding mode techniques have also been combined with disturbance observers and actuator-dynamic compensation to improve robustness and tracking precision [5]. In addition, several studies by Dinh and co-authors have shown that adaptive-gain and fast nonsingular terminal sliding mode strategies can significantly improve tracking performance in nonlinear motion systems such as

pneumatic artificial muscles and piezoelectric positioning stages [6-8]. These studies demonstrate the effectiveness of terminal sliding mode structures for high-precision nonlinear control problems.

Another important consideration in hydraulic motion systems is the pressure supply mechanism. Conventional constant-pressure hydraulic sources may cause unnecessary throttling losses when the required load pressure is lower than the fixed supply pressure. Load-sensing and pump-controlled hydraulic systems provide a practical way to improve energy usage by adjusting the supply pressure according to the actual load demand [9]. Therefore, it is meaningful to study position control of a servo-valve-controlled hydraulic rotary actuator supplied by a load-sensing pump.

This paper presents a terminal sliding mode controller for position tracking of a load-sensing electro-hydraulic rotary actuator. A simplified nonlinear model is first established by considering the main rotary mechanical dynamics, hydraulic pressure dynamics, valve-flow relation, servo-valve spool dynamics, and load-sensing supply-pressure regulation. Based on this model, a fixed-gain terminal sliding mode controller is developed to improve tracking response without increasing the controller structure unnecessarily. A continuous saturation function is used in the switching term to reduce chattering and improve control smoothness.

The main contributions of this paper are summarized as follows:

1. A simplified control-oriented nonlinear model of a servo-valve-controlled hydraulic rotary actuator with load-sensing pump supply is presented.
2. A terminal sliding mode controller is designed for angular position tracking.
3. The proposed controller is evaluated through MATLAB/Simulink simulations under sinusoidal, rectangular-wave, and chirp reference trajectories. Comparative results with PID and conventional sliding mode control are used to verify the tracking improvement of the terminal sliding mode controller.

The remainder of this paper is organized as follows. Section 2 describes the nonlinear model of the hydraulic rotary actuator system. Section 3 presents the terminal sliding mode controller design. Section 4 discusses the simulation results. Finally, Section 5 concludes the paper.

II. SYSTEM MODELING

To design the proposed controller, a simplified nonlinear model of the load-sensing hydraulic rotary drive is established. The system consists of a load-sensing pump, a servo valve, a rotary actuator, and a gear transmission connected to the output shaft. The servo valve regulates the hydraulic flow into the actuator chambers. The pressure difference between the two chambers produces the driving torque, and the gear set transfers the rotary motion to the load side.

Only the dominant dynamics are considered in the control-oriented model. The retained dynamics include the kinematic relation, load-pressure equation, servo-valve flow equation, rotary mechanical dynamics, valve-spool dynamics, and load-sensing supply-pressure relation. Friction uncertainty, leakage variation, and external load effects are treated as lumped disturbances.

The following assumptions are adopted.

A1. The rotary actuator is described by a two-chamber hydraulic model.

A2. The pressure response of the load-sensing pump is faster than the mechanical motion; therefore, the supply pressure can be approximated by an algebraic load-sensing relation.

A3. Friction uncertainty, leakage mismatch, parameter variation, and external load effects are grouped into lumped disturbance terms

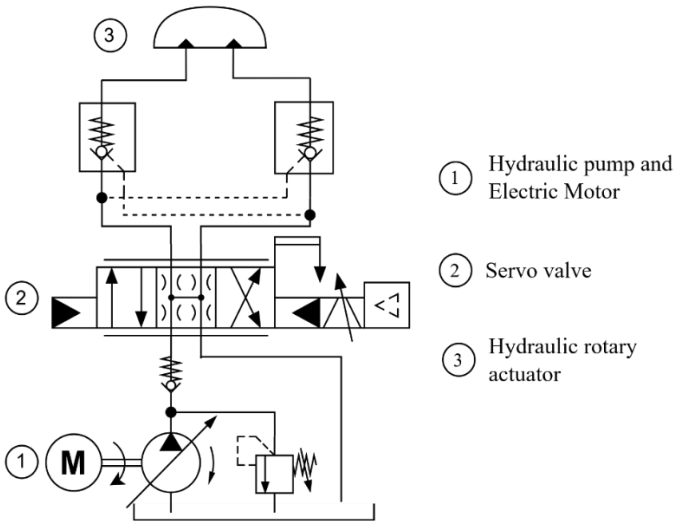

Figure 1. Schematic diagram of the hydraulic rotary actuator system

2.1 Kinematic Relation

The motor-side angular position and the load-side angular position are related through the gear ratio as

$$\theta_L = \frac{\theta_m}{N} \tag{1}$$

where $\theta_m$is the motor-side angular position, $\theta_L$is the load-side angular position, and $N$is the gear ratio.

The motor-side angular velocity is defined as

$$\omega_m = \dot{\theta}_m \tag{2}$$

The corresponding load-side angular velocity is obtained as

$$\dot{\theta}_L = \frac{\omega_m}{N} \tag{3}$$

2.2 Load Pressure and Hydraulic Flow

The load pressure is defined as the pressure difference between the two actuator chambers:

$$P_L = P_A - P_B \tag{4}$$

where P_A and $P_B$are the pressures in chambers A and B, respectively.

The load-pressure dynamics are written as

$$\dot{P}_L = \frac{4\beta_e}{V_t}(Q_L - D_m\omega_m - C_t P_L - Q_{\text{relief}}) \tag{5}$$

where β_e is the effective bulk modulus, $V_t$is the total trapped oil volume, Q_L is the load flow, D_m is the rotary actuator displacement coefficient, C_t is the internal leakage coefficient, and Q_{relief} is the relief-valve flow.

The servo-valve flow is modeled as

$$Q_L = C_v x_v \sqrt{P_s - \text{sgn}(x_v)P_L + \varepsilon} \tag{6}$$

where C_v is the valve-flow coefficient, $x_v$is the normalized spool displacement, P_s is the supply pressure, and ε is a small positive constant used to avoid numerical singularity.

The spool opening is bounded by

$$-1 \le x_v \le 1 \tag{7}$$

2.3 Rotary Mechanical Dynamics

The equivalent rotary motion referred to the motor side is described by

$$J_e\dot{\omega}_m = D_m P_L - B_e\omega_m - T_f - d_m \tag{8}$$

where $J_e$is the equivalent inertia, $B_e$is the equivalent viscous damping coefficient, $T_f$is the friction torque, and $d_m$is the lumped mechanical disturbance.

The equivalent inertia is expressed as

$$J_e = J_m + \frac{J_L}{\eta_g N^2} \tag{9}$$

The equivalent damping coefficient is

$$B_e = B_m + \frac{B_L}{\eta_g N^2} \tag{10}$$

where $J_m$and $B_m$are the motor-side inertia and damping coefficient, $J_L$and $B_L$are the load-side inertia and damping coefficient, and $\eta_g$is the transmission efficiency.

The friction torque is approximated by a smooth hyperbolic tangent function:

$$T_f = T_c\tanh\left(k_f\omega_m\right) \tag{11}$$

where $T_c$is the Coulomb friction level and $k_f$is a smoothing constant.

Substituting the friction model into the mechanical dynamics gives

$$J_e\dot{\omega}_m = D_m P_L - B_e\omega_m - T_c\tanh\left(k_f\omega_m\right) - d_m \tag{12}$$

2.4 Servo-Valve Dynamics

Since the valve spool cannot move instantaneously, the valve dynamics are represented by a second-order model:

$$\ddot{x}_v + 2\zeta_v\omega_v\dot{x}_v + \omega_v^2 x_v = K_v\omega_v^2 u \tag{13}$$

where $u$is the control voltage, $\omega_v$is the valve natural frequency, $\zeta_v$is the damping ratio, and $K_v$is the valve gain.

To simplify the state representation, define

$$z_v = \dot{x}_v$$

Then, the valve dynamics become

$$\begin{aligned} \dot{x}_v &= z_v \\ \dot{z}_v &= -2\zeta_v\omega_v z_v - \omega_v^2 x_v + K_v\omega_v^2 u \end{aligned} \tag{14}$$

2.5 Load-Sensing Supply Pressure

The load-sensing pump adjusts the supply pressure according to the instantaneous load demand. The supply-pressure law is written as

$$P_s = \min\left(P_{\max}, P_t + |\,P_L\,| + \Delta P_{LS}\right) \tag{15}$$

where $P_{\max}$is the maximum supply pressure, $P_t$is the tank pressure, and $\Delta P_{LS}$is the load-sensing pressure margin.

The supply pressure is constrained by

$$P_{\min} \le P_s(t) \le P_{\max} \tag{16}$$

This means that the pump does not always operate at the maximum pressure. Instead, it provides only the pressure level required by the load plus the pressure margin.

2.6 State-Space Form

Choose the state variables as $x_1 = \theta_m, x_2 = \omega_m, x_3 = P_L, x_4 = x_v, x_5 = z_v$

Thus, the state vector is

$$x = [x_1 \quad x_2 \quad x_3 \quad x_4 \quad x_5]^T \tag{17}$$

Using the above equations, the simplified state model is written as

$$\begin{aligned} \dot{x}_1 &= x_2 \\ \dot{x}_2 &= \frac{D_m x_3 - B_e x_2 - T_c \tanh(k_f x_2) - d_m}{J_e} \\ \dot{x}_3 &= \frac{4\beta_e}{V_t}(Q_L - D_m x_2 - C_t x_3 - Q_{\text{relief}}) \\ \dot{x}_4 &= x_5 \\ \dot{x}_5 &= -2\zeta_v \omega_v x_5 - \omega_v^2 x_4 + K_v \omega_v^2 u \end{aligned} \tag{18}$$

where the flow term becomes

$$Q_L = C_v x_4 \sqrt{P_s - \text{sgn}(x_4) x_3 + \varepsilon} \tag{19}$$

and the supply pressure is rewritten as

$$P_s = \min(P_{\max}, P_t + | x_3 | + \Delta P_{LS}) \tag{20}$$

2.7 Control Objective

The control input is the valve voltage u, and the controlled output is the load-side angle θ_L. The load-side tracking error is defined as

$$e_L = \theta_L - \theta_d \tag{21}$$

where $\theta_d$is the desired angular position.

Using the gear relation, the motor-side tracking error can also be written as

$$e_m = \theta_m - N\theta_d \tag{22}$$

The desired closed-loop requirements are summarized as

$$\begin{aligned} | x_v(t) | &\leq 1 \\ e_L(t) &\to \Omega_e \\ | u(t) | &\leq u_{\max} \\ P_{\min} \leq P_s(t) &\leq P_{\max} \end{aligned} \tag{23}$$

where Ω_e denotes a small neighborhood around the origin. These requirements indicate that the controller should achieve accurate tracking while keeping the voltage input, spool motion, and hydraulic pressure within allowable limits.

III. TERMINAL SLIDING MODE CONTROLLER DESIGN

This section develops a terminal sliding mode controller for the load-sensing hydraulic rotary actuator. The main objective is to force the load-side angular position to follow a prescribed reference trajectory with fast convergence and strong robustness. Since the mathematical model is expressed in motor-side coordinates, the desired load-side trajectory is first converted into the corresponding motor-side reference.

3.1 Tracking Error Definition

Let θ_d denote the desired load-side angular position. Based on the gear ratio, the corresponding desired motor-side position is defined as $\theta_{md} = N\theta_d$

The motor-side tracking error is selected as

$$e_m = x_1 - \theta_{md} \tag{24}$$

Taking the first derivative of the tracking error gives

$$\dot{e}_m = x_2 - \dot{\theta}_{md} \tag{25}$$

The second derivative of the tracking error is obtained as

$$\ddot{e}_m = \dot{x}_2 - \ddot{\theta}_{md} \tag{26}$$

where θ_{md}, $\dot{\theta}_{md}$, and $\ddot{\theta}_{md}$ are the desired motor-side position, velocity, and acceleration, respectively.

3.2 Terminal Sliding Surface

To improve both transient response and near-origin convergence, the terminal sliding surface is chosen as

$$s = \dot{e}_m + \lambda e_m + \alpha | e_m |^{p/q} \text{sgn}(e_m) \tag{27}$$

where $\lambda$and $\alpha$are positive design gains. The constants $p$and $q$are positive odd integers satisfying

$$0 < \frac{p}{q} < 1 \tag{28}$$

The term λe_mimproves the general convergence response, whereas the nonlinear terminal term $\alpha \mid e_m \mid^{p/q} \operatorname{sgn}(e_m)$accelerates convergence when the tracking error approaches zero.
The time derivative of the sliding surface is

$$\dot{s} = \ddot{e}_m + \lambda \dot{e}_m + \alpha \frac{p}{q} \mid e_m \mid^{p/q-1} \dot{e}_m \tag{29}$$

Substituting (26) into (29) yields

$$\dot{s} = \dot{x}_2 - \ddot{\theta}_{md} + \lambda \dot{e}_m + \alpha \frac{p}{q} \mid e_m \mid^{\frac{p}{q}-1} \dot{e}_m \tag{30}$$

From the mechanical dynamics of the hydraulic rotary actuator, the motor-side angular acceleration is

$$\dot{x}_2 = \frac{D_m x_3 - B_e x_2 - T_c \tanh(k_f x_2) - d_m}{J_e} \tag{31}$$

Therefore, the sliding surface dynamics can be written as

$$\dot{s} = \frac{D_m x_3 - B_e x_2 - T_c \tanh(k_f x_2) - d_m}{J_e} - \ddot{\theta}_{md} + \lambda \dot{e}_m + \alpha \frac{p}{q} \mid e_m \mid^{\frac{p}{q}-1} \dot{e}_m \tag{32}$$

3.3 Desired Load Pressure

The load pressure $P_L$is considered as a virtual control input for the mechanical subsystem. To drive the sliding variable toward zero, the desired sliding dynamics are selected as

$$\dot{s} = -k_s s - \eta \operatorname{sat}\left(\frac{s}{\phi}\right) \tag{33}$$

where $k_s$is a positive feedback gain, $\eta$is a positive switching gain, and $\phi$is the boundary-layer thickness.
The saturation function is defined by

$$\operatorname{sat}\left(\frac{s}{\phi}\right) = \begin{cases} \frac{s}{\phi} \; if \mid \frac{s}{\phi} \mid \leq 1 \\ \operatorname{sgn}\left(\frac{s}{\phi}\right) \; otherwise \end{cases} \tag{34}$$

Using (31) and (32), the desired load pressure is obtained as

$$P_{Ld} = \frac{1}{D_m}\left[J_e \ddot{\theta}_{md} + B_e x_2 + T_c \tanh(k_f x_2) - J_e \lambda \dot{e}_m - J_e \alpha \frac{p}{q} \mid e_m \mid^{\frac{p}{q}-1} \dot{e}_m - J_e k_s s - J_e \eta \operatorname{sat}\left(\frac{s}{\phi}\right)\right] \tag{35}$$

where $P_{Ld}$is the desired load pressure. The terms $J_e \ddot{\theta}_{md}$, $B_e \dot{\theta}_m$, and $T_f$compensate for the desired acceleration, viscous damping, and friction, respectively. The remaining terms enforce the desired terminal sliding dynamics.
To avoid excessive pressure demand, the desired load pressure is bounded by

$$P_{Ld} = \operatorname{sat}(P_{Ld}, -P_{L\max}, P_{L\max})$$

where $P_{L\max}$ is the maximum allowable load pressure.

3.4 Pressure Tracking Control

The pressure tracking error is defined as

$$e_p = x_3 - P_{Ld} \tag{36}$$

The load-pressure dynamics are given in (5). In order to make $P_L$follow P_{Ld}, the desired load flow is designed as

$$Q_{Ld} = D_m x_2 + C_t x_3 + Q_{relief} + \frac{V_t}{4\beta_e}\left(\dot{P}_{Ld} - k_p e_p\right) \tag{37}$$

where $k_p$is a positive pressure-loop gain, and $Q_{Ld}$is the desired load flow.
Substituting (37) into (36) gives the ideal pressure error dynamics

$$\dot{e}_p = -k_p e_p \tag{38}$$

Thus, the pressure tracking error converges to a small neighborhood of zero if the desired load flow can be accurately generated by the servo valve.

3.5 Desired Valve Spool Position

By inverting the flow relation, the desired spool displacement is obtained as

$$x_{vd} = \frac{Q_{Ld}}{C_v \sqrt{P_S - \operatorname{sgn}(Q_{Ld}) x_3 + \varepsilon}} \tag{39}$$

where $x_{vd}$is the desired normalized spool displacement.

3.6 Valve Spool Control

The valve spool tracking error is defined as

$$e_v = x_4 - x_{vd} \tag{40}$$

The derivative of the spool tracking error is

$$\dot{e}_v = x_5 - \dot{x}_{vd} \tag{41}$$

To make $x_v$follow x_{vd}, the desired valve-spool error dynamics are selected as

$$\ddot{e}_v + k_v \dot{e}_v + k_x e_v = 0 \tag{42}$$

where $k_v$and $k_x$are positive valve-loop gains.

From the servo valve dynamics (13), equations (41) and (42), the valve input voltage is designed as $u = \frac{\ddot{x}_{vd}+2\zeta_v\omega_v x_5+\omega_v^2 x_4-k_v\dot{e}_v-k_x e_v}{K_v\omega_v^2}$ (43)

where $\dot{x}_{vd}$and $\ddot{x}_{vd}$are the first and second derivatives of the desired spool displacement.

To satisfy the voltage limit of the servo-valve amplifier, the final control input is constrained by

$$u = \mathrm{sat}(u, -u_{\max}, u_{\max}) \quad (44)$$

where $u_{\max}$ is the maximum allowable valve voltage. The terminal sliding surface improves the convergence rate of the tracking error, while the saturation function replaces the discontinuous sign function to reduce chattering in the pressure command and valve input.

IV. NUMERICAL EVALUATION AND DISCUSSION

4.1 Simulation Conditions and Evaluation Indices

Numerical simulations were performed in MATLAB/Simulink to verify the tracking capability of the terminal sliding mode controller. The plant model was constructed from the nonlinear hydraulic rotary actuator model described in Section 2, including rotary mechanical dynamics, load-pressure dynamics,

nonlinear servo-valve flow, valve-spool dynamics, friction, internal leakage, and load-sensing pressure regulation.

Three controllers were considered for comparison: a PID controller, a conventional sliding mode controller, and the proposed terminal sliding mode controller. The PID controller was used as a basic industrial benchmark. The conventional SMC was included to evaluate the benefit of robust switching control, while the TSMC was used to improve the convergence behavior of the tracking error through a nonlinear terminal sliding surface.

The simulations were conducted under three reference trajectories: sinusoidal reference, rectangular-wave reference, and chirp reference. The disturbance case was not included in this simplified study. Therefore, the comparison mainly focuses on nominal tracking accuracy, transient response, frequency adaptability, and smoothness of the control input.

The control voltage was also examined because high-frequency oscillations in the valve input may excite spool vibration, pressure ripple, mechanical vibration, and unnecessary hydraulic energy loss.

4.2 Smooth Periodic Tracking Test

The sinusoidal reference trajectory was employed to assess the steady-state periodic tracking capability of the three controllers. Since the reference signal varies smoothly with time, this case mainly evaluates phase deviation, amplitude attenuation, and steady tracking accuracy under continuous motion.

As shown in Fig. 2, the PID controller is able to reproduce the general sinusoidal response. However, its tracking error remains comparatively large. This limitation is mainly caused by the fixed-gain structure of the PID controller, which cannot sufficiently compensate for the nonlinear pressure dynamics, valve-flow characteristics, friction effect, and coupled hydraulic-mechanical behavior of the actuator. In particular, when the reference velocity increases, a noticeable phase lag appears in the tracking response.

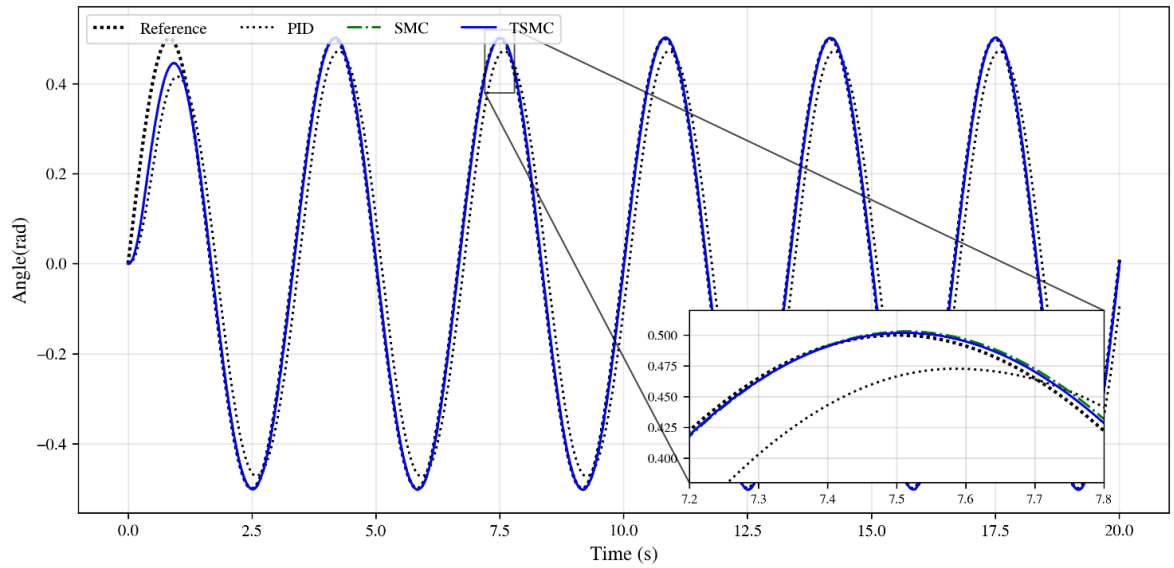

Figure 2. Tracking performances with respect to sinusoidal reference

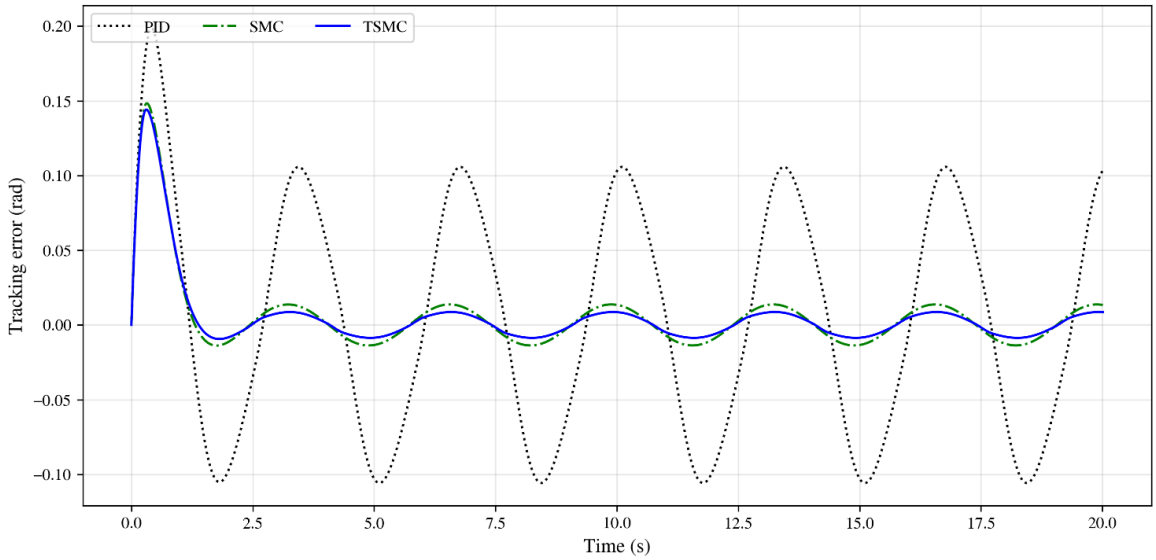

Figure 3. Tracking errors with respect to sinusoidal reference

The conventional SMC improves the tracking performance compared with the PID controller. This improvement is obtained because the switching component enhances robustness against model uncertainty and nonlinear system effects. Nevertheless, the control voltage generated by SMC exhibits more oscillatory behavior. This is a typical consequence of the switching action, which may change rapidly when the system trajectory approaches and crosses the sliding surface.

As illustrated in Fig. 3, the proposed TSMC achieves the smallest tracking error among the three controllers in the sinusoidal tracking case. The nonlinear terminal term in the sliding surface

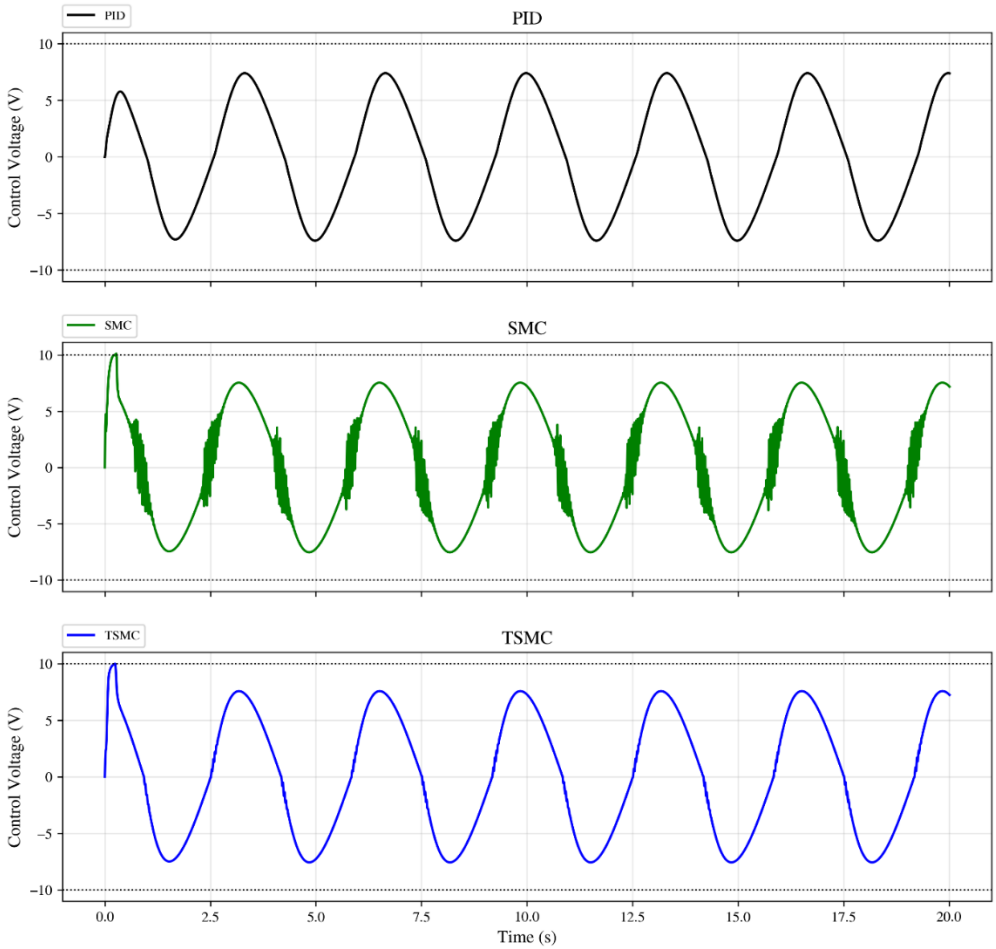

Figure 4. Control voltages with respect to sinusoidal reference

accelerates the convergence of the tracking error, especially when the system state is close to the desired trajectory. Therefore, the proposed controller provides improved tracking accuracy compared with both PID and conventional SMC. In addition, the control voltage response in Fig. 4 shows that the proposed TSMC produces less chattering than the conventional SMC, indicating a better balance between tracking performance and control smoothness.

4.3 Transient Response Under Rectangular Reference

The rectangular-wave reference trajectory was used to examine the transient response of the controllers under abrupt position changes and repeated motion reversals. This case is more demanding than sinusoidal tracking because the reference contains sudden transitions, which require fast error convergence and good overshoot suppression. Fig. 5 presents the tracking performances of the three

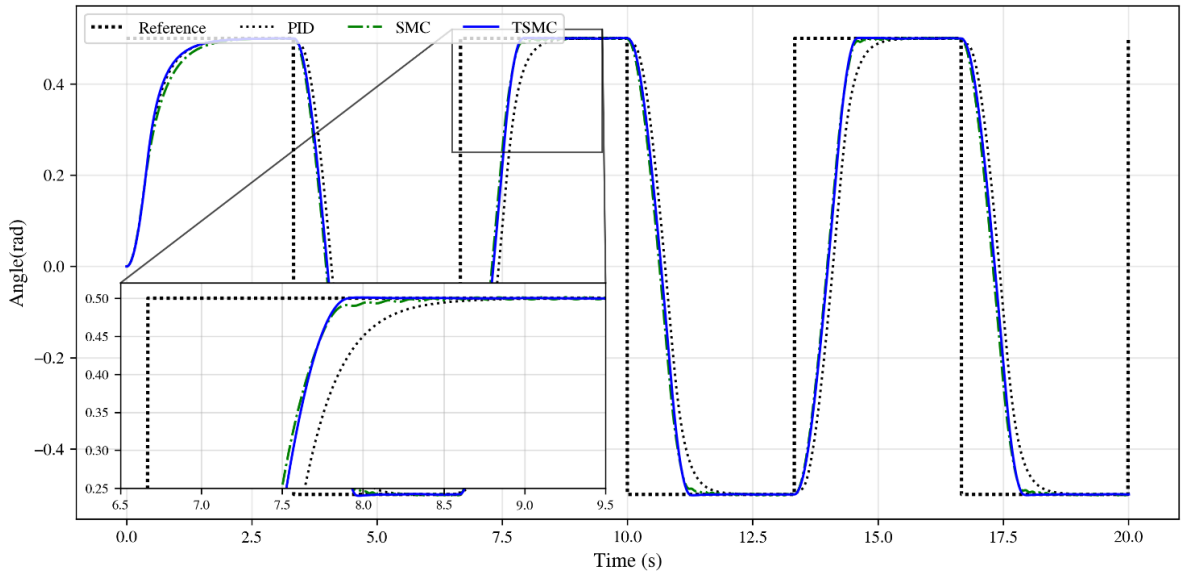

Figure 5. Tracking performances with respect to rectangular wave reference

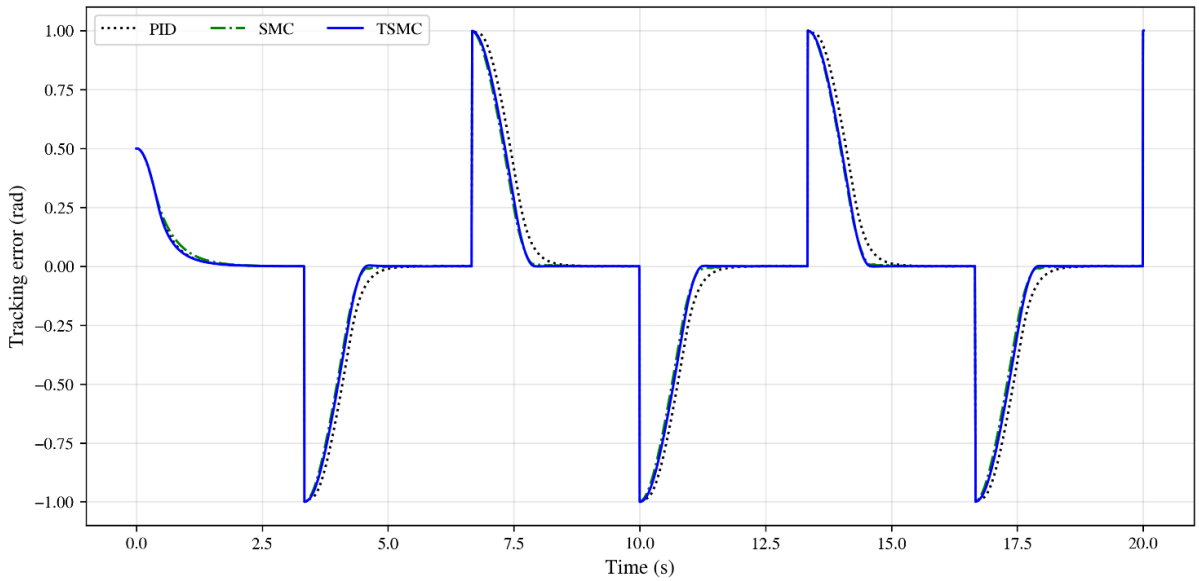

Figure 6. Tracking errors with respect to rectangular wave reference

controllers, Fig. 6 shows the corresponding tracking errors, and Fig. 7 illustrates the control voltage signals.

As shown in Fig. 5, the PID controller exhibits a relatively slow transient response after each reference change. In addition, larger overshoot can be observed around the transition instants. This behavior is mainly due to the fixed-gain linear structure of the PID controller, which does not directly compensate for the nonlinear pressure dynamics, valve-flow characteristics, friction effect, and hydraulic-mechanical coupling of the actuator. Therefore, it is difficult to simultaneously obtain fast response and small overshoot through PID gain tuning alone.

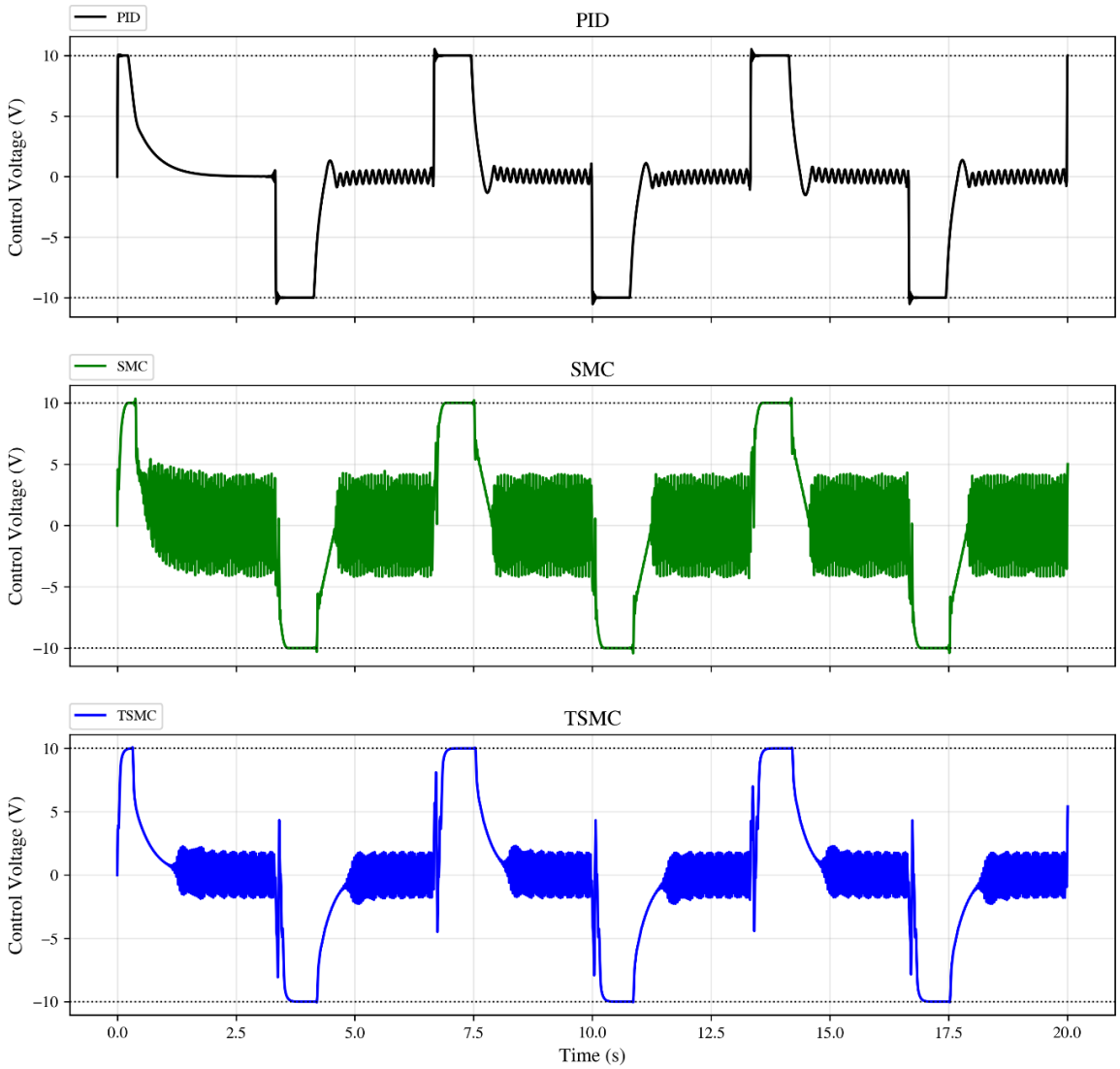

Figure 7. Control voltages with respect to rectangular wave reference

From the tracking error comparison in Fig. 6, the conventional SMC reduces the convergence time compared with PID because its switching term improves robustness against nonlinearities and modeling uncertainties. However, as shown in Fig. 7, the control voltage generated by SMC contains noticeable high-frequency oscillations during the constant intervals of the rectangular reference. This chattering phenomenon occurs because the sliding variable repeatedly moves around the neighborhood of the sliding surface, causing frequent switching in the control action.

The proposed TSMC provides better transient tracking performance than both PID and conventional SMC. After each reference transition, the output settles faster and the tracking error is reduced more effectively, as confirmed by Fig. 5 and Fig. 6. This improvement is achieved by the nonlinear terminal sliding surface, which strengthens the convergence behavior when the tracking error approaches the equilibrium region. Moreover, Fig. 7 shows that the control voltage generated by the proposed TSMC has less chattering than that of the conventional SMC. This indicates that the proposed controller can improve transient accuracy while maintaining a smoother valve command, which is beneficial for reducing spool vibration and pressure oscillation in hydraulic systems.

V. CONCLUSION

This study investigated the position tracking control problem of a servo-valve-controlled electro-hydraulic rotary actuator supplied by a load-sensing pump. A simplified nonlinear model was first constructed by considering the dominant mechanical motion, load-pressure variation, valve-flow characteristic, servo-valve spool response, and load-sensing supply-pressure relation. Based on this model, a terminal sliding mode controller was developed for angular position tracking. The proposed controller uses a nonlinear terminal sliding surface to improve the convergence behavior of the tracking error. To make the control signal more suitable for hydraulic

implementation, a continuous saturation function was employed instead of the ideal sign function. This modification helps reduce high-frequency switching in the valve command, which is important for limiting spool vibration, pressure ripple, and chattering-related effects.

Simulation studies were carried out under sinusoidal, rectangular-wave, and chirp reference trajectories. The results showed that the PID controller provided the simplest structure but produced larger tracking errors, especially during fast motion changes. The conventional sliding mode controller improved tracking performance but generated more noticeable switching oscillations. Compared with these two controllers, the terminal sliding mode controller achieved better tracking accuracy and faster transient response while maintaining an acceptable control effort.

REFERENCES

[1]. J. Yao, Z. Jiao, D. Ma, and L. Yan, "High-Accuracy Tracking Control of Hydraulic Rotary Actuators With Modeling Uncertainties," IEEE/ASME Transactions on Mechatronics, vol. 19, no. 2, pp. 633–641, 2014.

[2]. J. Mattila, J. Koivumäki, D. G. Caldwell, and C. Semini, "A Survey on Control of Hydraulic Robotic Manipulators With Projection to Future Trends," IEEE/ASME Transactions on Mechatronics, vol. 22, no. 2, pp. 669–680, 2017.

[3]. Z. Man and Y. Huo, "Terminal Sliding Mode Control of MIMO Linear Systems," IEEE Transactions on Circuits and Systems I: Fundamental Theory and Applications, vol. 44, no. 11, pp. 1065–1070, 1997.

[4]. Y. Feng, X. Yu, and Z. Man, "Non-Singular Terminal Sliding Mode Control of Rigid Manipulators," Automatica, vol. 38, no. 12, pp. 2159–2167, 2002.

[5]. T. X. Dinh, T. D. Thien, T. H. V. Anh, and K. K. Ahn, "Disturbance Observer Based Finite Time Trajectory Tracking Control for a 3 DOF Hydraulic Manipulator Including Actuator Dynamics," IEEE Access, vol. 6, pp. 36798–36809, 2018.

[6]. C. P. Vo, X. D. To, and K. K. Ahn, "A Novel Adaptive Gain Integral Terminal Sliding Mode Control Scheme of a Pneumatic Artificial Muscle System With Time-Delay Estimation," IEEE Access, vol. 7, pp. 141133–141143, 2019.

[7]. T. X. Dinh and K. K. Ahn, "Radial Basis Function Neural Network Based Adaptive Fast Nonsingular Terminal Sliding Mode Controller for Piezo Positioning Stage," International Journal of Control, Automation and Systems, vol. 15, pp. 2892–2905, 2017.

[8]. T. X. Dinh and K. K. Ahn, "Adaptive-Gain Fast Nonsingular Terminal Sliding Mode for Position Control of a Piezo Positioning Stage," Proceedings of the Institution of Mechanical Engineers, Part I: Journal of Systems and Control Engineering, vol. 232, no. 8, pp. 994–1014, 2018.

[9]. C. Li, L. Lyu, B. Helian, Z. Chen, and B. Yao, "Precision Motion Control of an Independent Metering Hydraulic System With Nonlinear Flow Modeling and Compensation," IEEE Transactions on Industrial Electronics, vol. 69, no. 7, pp. 7088–7097, 2022.